Supporting Information

Single-crystalline Sb_2S_3 Tubes for High-Performance Broadband Visible Photodetection

Shili Fu [a,+], Xiaohui Liu [a,+], Haoyun Dou [a,+], Rawaid Ali [a], Ao Zeng [a], Jiaxiu Man [a], Xiaolu Zheng [a,*], Hong-En Wang [a,b,*]

[a] College of Physics and Electronic Information, Yunnan Normal University, 650500 Kunming, China. E-mail: hongen.wang@ynnu.edu.cn, inkzheng@foxmail.com

[b] Yunnan Key Laboratory of Optoelectronic Information Technology, Yunnan Normal University, 650500 Kunming, China. E-mail: hongen.wang@outlook.com

[+] These authors contributed equally to this work.

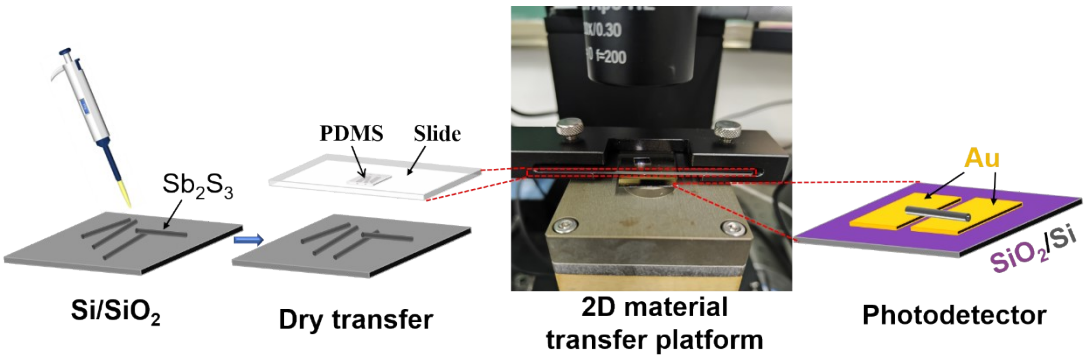

Figure S1. Schematic illustration of the fabrication process of the Sb_2S_3 microtube-based photodetector device. PDMS: polydimethylsiloxane

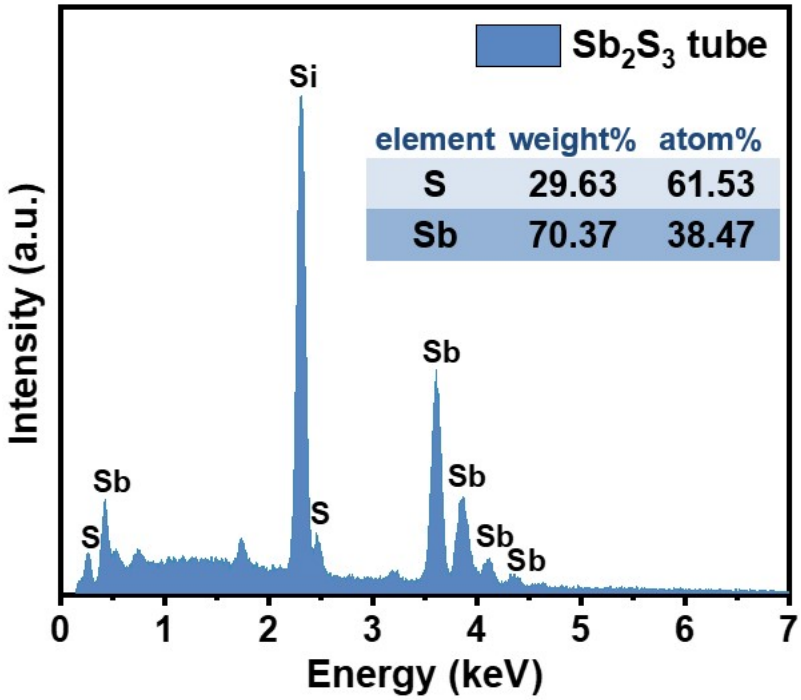

Figure S2. Energy-dispersive X-ray spectroscope spot images of Sb_2S_3, the inset shows the weight and atomic information for each element.

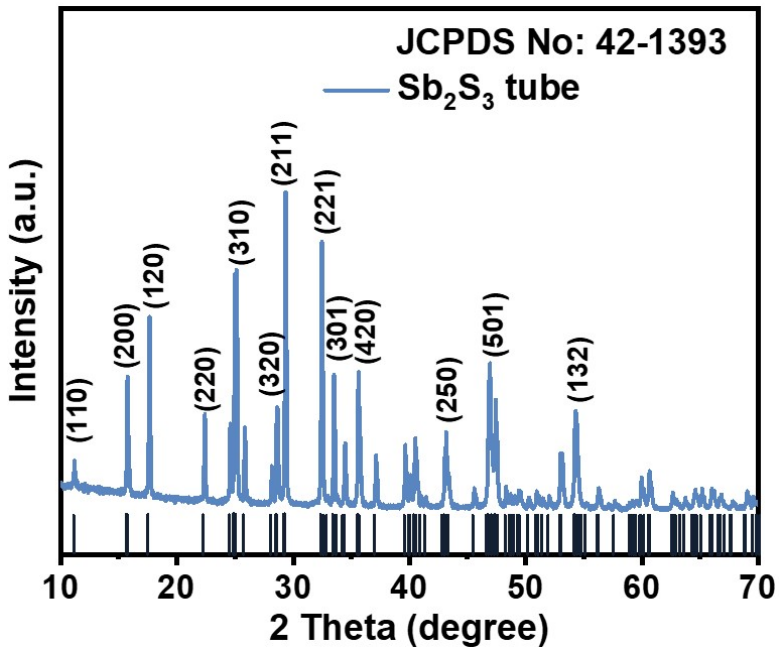

Figure S3. X-ray diffraction pattern of the as-synthesized Sb_2S_3 microtubes.

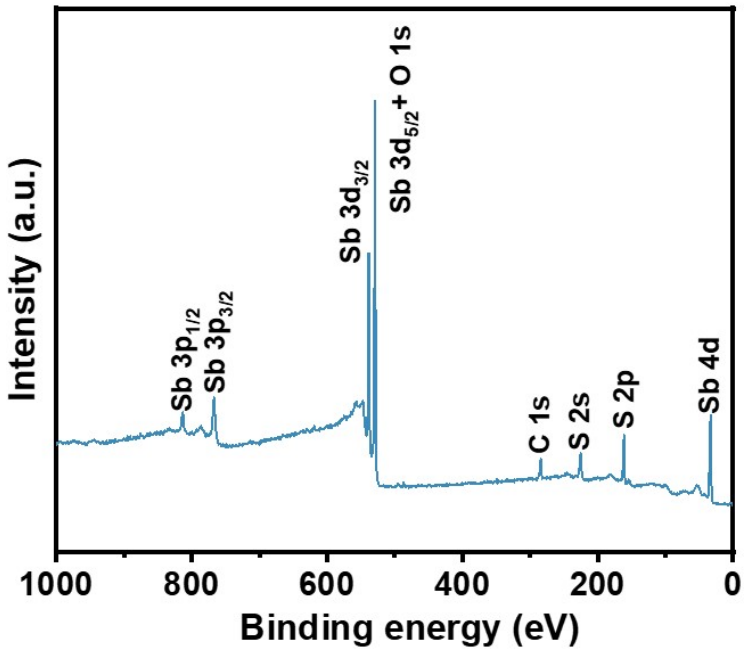

Figure S4. Survey X-ray photoelectron spectroscopy spectrum of the as-received Sb_2S_3 microtubes.

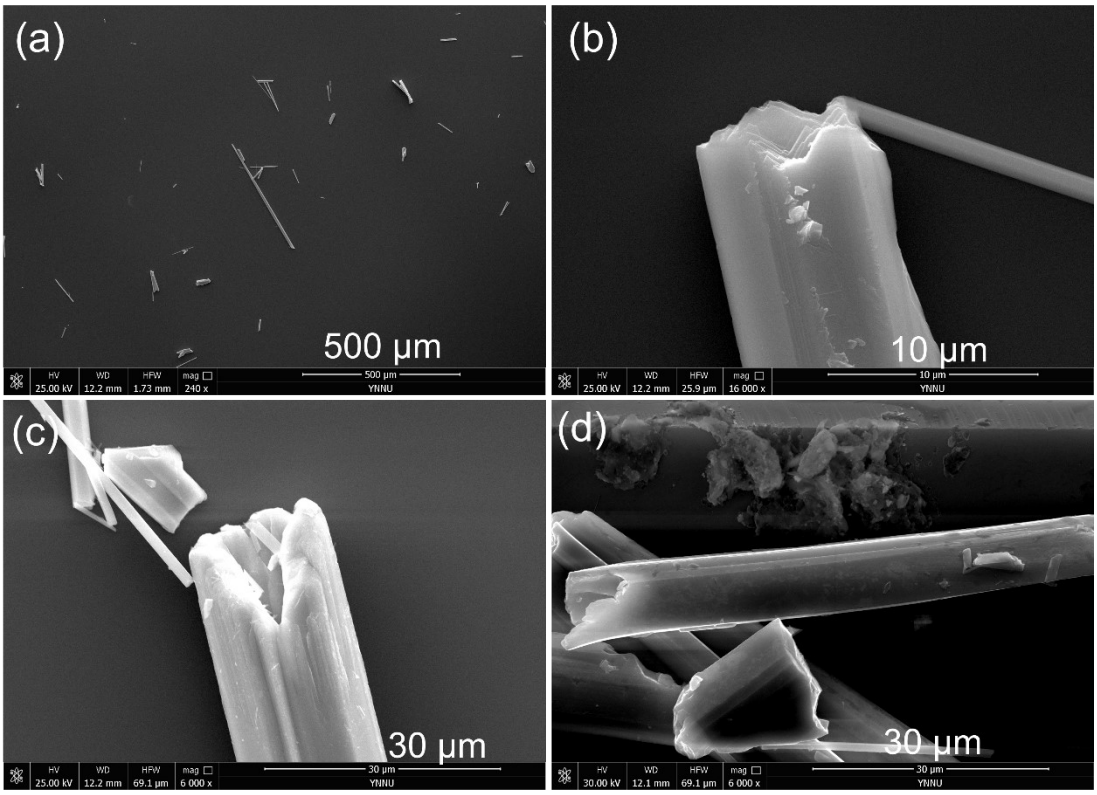

Figure S5. SEM images of the Sb_2S_3 products synthesized after hydrothermal reaction for 24 h with the addition of different amounts of EDTA: (a, b) 1 mmol, (c) 3 mmol, and (d) 4 mmol.

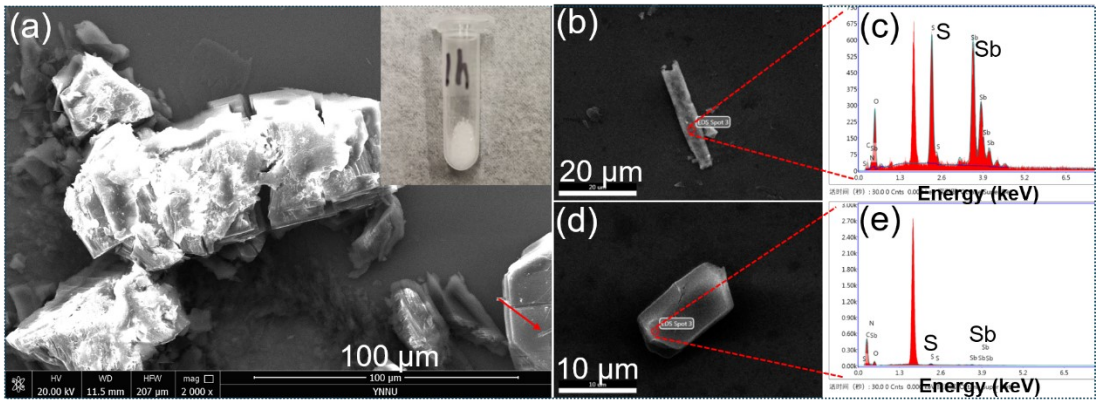

Figure S6. SEM images (a, b, and d) and EDX spectra (c, e) of the product synthesized by hydrothermal reaction for 1 h.

SEM image (Figure S6a) reveals the product obtained after hydrothermal reaction for 1 h mainly consists of some irregular aggregates with size larger than 100 μm. Only a very small amount of microrods was produced, as indicated by the red arrow in Figure R1a. An additional SEM image of one microrod (Figure S6b) and the corresponding EDX spectrum (Figure S6c) unravel it mainly consists of Sb and S elements with an atomic ratio of approximately 0.93. In contrast, the SEM image (Figure S6d) and the associated EDX spectrum (Figure S6e) reveal that the irregular large microparticles are almost free of Sb/S and are primarily composed of an unknown intermediate product consisting of some C, N, and O elements. This result is consistent with the very bright image in Figure S6a (mainly caused by poor conductivity of the sample surface leading to discharge during SEM testing). Meantime, the digital photograph (inset, Figure S6a) also shows that the amount of product collected is minimal and appears white. This observation discloses that the reaction for the synthesis of Sb_2S_3 in 1 h is incomplete.

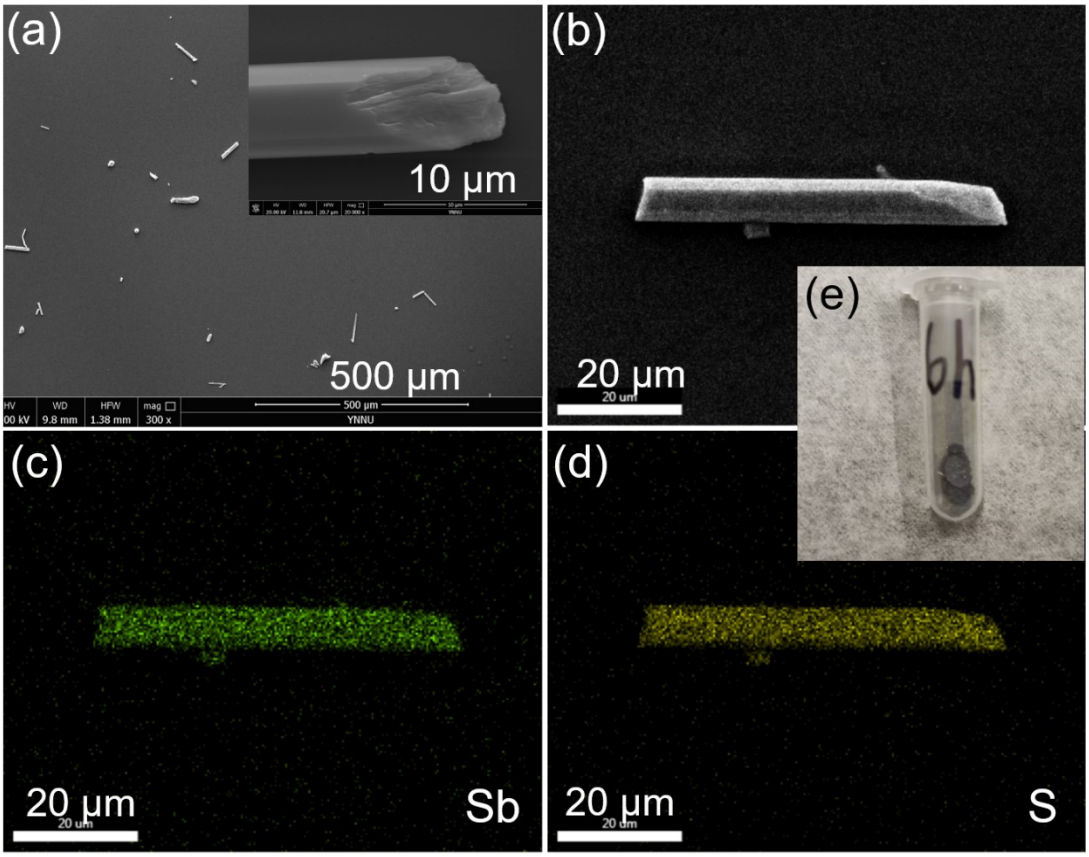

Figure S7. SEM images (a, b) and EDX mapping images (c, d), and (e) an optical photo of the product synthesized by hydrothermal reaction for 6 h.

From Figure S7a that in the product synthesized by hydrothermal reaction for 6 h, the amount of microrods has significantly increased, in addition to the large particles with irregular shapes. The SEM image in Figure S7b, along with the corresponding EDX mapping images in Figures S7c and S7d, shows a single microrod composed of Sb and S. The elements are uniformly distributed with an atomic ratio of approximately 0.59, confirming the microrod to be Sb_2S_3. In addition, the optical photo of the sample also appears as dark grey, consistent with the color of Sb_2S_3.

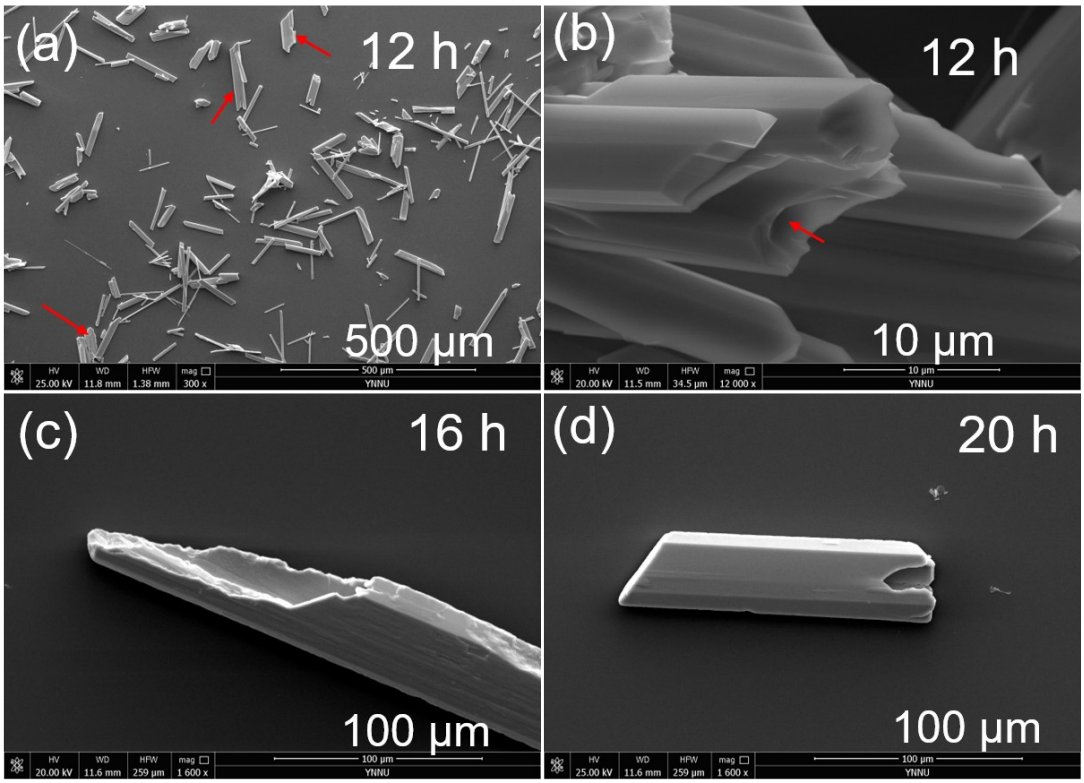

Figure S8. SEM images of the Sb_2S_3 products synthesized by hydrothermal reaction for different durations: (a, b) 12 h, (c) 16 h, and (d) 20 h.

SEM image (Figure S8a) reveals that extending the reaction time to 12 h, the resulting sample contains many microrods; simultaneously, some flattened microbelts are formed (as indicated by the red arrows), which may be caused by oriented attachment between the microrods. From the high-magnification SEM image in Figure S8b, these microrods do not yet display a hollow structure, but they do show a tendency to start hollowing out (as indicated by the red arrow). However, for samples reacted for 16 h and 20 h, there is a clear formation of microtubes, as shown in Figures S8c and S8d.

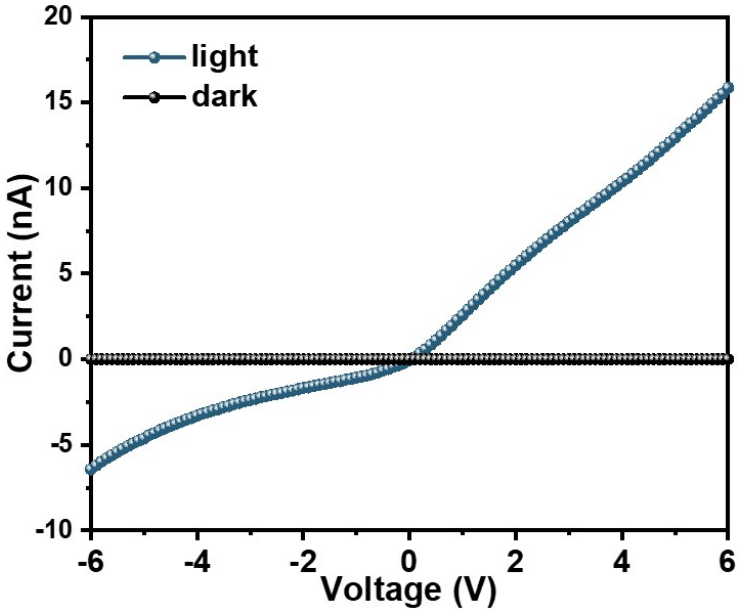

Figure S9. *I-V* plot of the device in natural light with a bias voltage of 6 V

Table S1. Adsorption energy and surface energy of Sb_2S_3 on different surfaces

Sb_2S_3 slab	X(Å)	Y(Å)	A(Å)	$E_{surface}$ (eV)	*Eads* (eV)
(001)	11.12	11.47	127.55	0.023	-0.74
(010)	3.86	11.12	42.92	0.030	-0.55
(100)	11.47	3.86	44.27	0.027	-0.64

Table S2. photodetection property comparison of our work with recent literature

Device structure	**λ (nm)**	$R_\lambda(A\,W^{-1})$	***EQE*** (%)	D^* **(Jones)**	**Rise/decay (ms)**	**Refs.**
Sb_2S_3 film	530	0.035	-	3.18×10^{10}	23.2/58	1
TiO_2/Sb_2S_3	530	0.057	-	5.30×10^{10}	0.6/11.8	1
Sb_2S_3 microrods	560	5.10	1130.68	2.16×10^{10}	4.03/4.08	2
Sb_2S_3 nanowires	532	65	1.5×10^4	2.1×10^{14}	76/82	3
Sb_2S_3 tubes	808	0.0085	-	1.33×10^6	22/24	4
Sb_2S_3/PbI_2	445	156.3	4.4×10^4	3.2×10^{13}	8.5/8.7	5
Sb_2S_3/PbI_2	730	120.74	2.06×10^4	2.45×10^{12}	-	5
Sb_2Se_3 NTs	830	4.39	655	9.63×10^{10}	27/27	6
Sb_2S_3 microtubes	**722**	**28.99**	**13021**	**7.6×10^{10}**	**9.8/9.2**	**This work**

Reference

1 Y. Jia, H. Deng, X. Lin, S. Chen, Y. Xia, Z. Wu, J. Yu, S. Cheng and Y. Lai, Depleted Sb_2S_3 Thin Film Photoconductive Detectors with Fast Response Speed and High Polarization Sensitivity, *Adv. Mater. Interfaces*, 2022, **9**, 2101504.

2 X. Liu, S. Dong, X. Zheng, Y. Zhang, Y. Yao, W. Zhang, Z. Liu, T. Zhu, and H. Wang, Improving the optoelectronic properties of single-crystalline antimony sulfide rods through simultaneous defect suppression and surface cleaning, *J. Mater. Chem. A*, 2023, **11**, 8826-8835.

3 K. Ye, B. Wang, A. Nie, K. Zhai, F. Wen, C. Mu, Z. Zhao, J. Xiang, Y. Tian, Z. Liu, Broadband photodetector of high quality Sb_2S_3 nanowire grown by chemical vapor deposition, *J. Mater. Sci. Tech.*, 2021, **75**, 14–20.

4 J. Zhang, K. Hou, T. Huang, J. Yang, B. Xu, S. Li, B. Yang, W. Ma, Single-crystal Sb_2S_3 tube prepared by chemical vapor deposition for a 1 cm photodetector application, *ACS Appl. Electron. Mater.*, 2022, **4**, 2455–2462.

5 S. Fu, X. Liu, J. Man, Q. Ou, X. Zheng, Z. Liu, Ting Zhu and Hong-En Wang 2D/1D PbI_2/Sb_2S_3 van der Waals heterojunction for highly sensitive and broadband photodetectors, *J. Mater. Chem. C*, 2024, **12**, 3353-3364.

6 S. Zhang, H. Wang, W. Pan, H. Luo, Y. Ren, Y. Liang, J. Tan, C. Yuan, W. Lei, Polarization-sensitive near-infrared photodetectors based on quasi-one-dimensional Sb_2Se_3 nanotubes, *J. Alloy. Compd.*, 2023, **937**, 168284.